Laser Physics Letters

Astro Ltd.

OPEN ACCESS

RECEIVED
7 October 2025

ACCEPTED FOR PUBLICATION
9 December 2025

PUBLISHED
6 February 2026

LETTER

Memory and correlation impacts in 3D-Pauli-like noisy channels for controlled teleportation of arbitrary single-qutrit states

Miao Liu[1,3,4], **Nueraminaimu Maihemuti**[2,4], **Jia-yin Peng**[1,2,3,*] **and Yimamujiang Aisan**[2]

[1] The School of Mathematics and Statistics, Yili Normal University, Xinjiang, Yili 835000, People's Republic of China
[2] School of Mathematics and Statistics, Kashi University, Xinjiang, Kashi 844000, People's Republic of China
[3] Current address: Institute of Applied Mathematics, Yili Normal University, Xinjiang, Yili 835000, People's Republic of China.
[4] Co-first authors. These authors contributed equally to this work.
[*] Author to whom any correspondence should be addressed.

E-mail: pengjiayin62226@163.com

Keywords: three-dimensional quantum teleportation, controlled quantum, fidelity, 3D-Pauli-like noise, memory channel

Abstract

The purpose of this paper is to further investigate the correlated and memory effects in 3D-Pauli-like noisy channels for controlled teleportation of an arbitrary unknown single-qutrit state. We first construct a three-qutrit maximally entangled state in a three-dimensional (3D) Hilbert space and subsequently propose a 3D controlled quantum teleportation (CQT) scheme for an arbitrary unknown single-qutrit state using the constructed three-qutrit maximally entangled state as the quantum channel. In this ideal case, through a few simple 3D unitary operations, the two communicating parties can perfectly accomplish the teleportation task under the supervision of the controller. Subsequently, we examine the performance of this CQT scheme under two successive uses of a 3D-Pauli-like noisy channel with memory, where the noise errors are categorized into four types: trit-flip, t-phase-flip, trit-phase-flip, and t-depolarizing. For each noise type, an analytical expression of the average fidelity is derived as a function of both the noise and memory parameters. Specifically, we find that, regardless of the noise strength, memory enhances the average fidelity for trit-flip and t-depolarizing noises, whereas for t-phase-flip and trit-phase-flip noises, memory reduces the average fidelity once the noise intensity exceeds a certain threshold. This indicates that in the first two noisy channels, memory can improve the communication efficiency of CQT, while in the latter two, excessive noise causes memory to diminish the teleportation performance.

1. Introduction

Quantum information science has made great progress over the past 30 years. As a significant part of quantum information science research, quantum communication theory and technology have made significant breakthroughs [1–7]. Based on the quantum cryptography system composed of a single photon source and optical fiber channel, communication between two nodes separated by hundreds of kilometers can be realized. However, the communication distance and performance are limited by geographical conditions, fiber attenuation, and the weak energy of single photons, among other factors. To overcome these limitations, quantum entanglement has emerged as a highly promising solution. In fact, the study of entangled states has been ongoing. In 1982, the phenomenon of quantum entanglement was successfully confirmed by Aspect *et al* through experiments [8]. The concept of quantum teleportation (QT) was first proposed by Bennett *et al* [9] in 1993. The feasibility of QT has also been verified by several physical experiments [10, 11]. Subsequently, quantum entanglement-based communication has attracted extensive attention. A large number of QT schemes using multi-qubit entangled states have been presented, such as the W state [12], GHZ state [13], four-qubit [14], five-qubit [15], and six-qubit [16] entangled states. The CQT [17] protocol enhances the security of QT by requiring a controller to authorize the transmission between the sender and receiver. Bidirectional QT protocols have

been developed [15–18], enabling both the sender and receiver to exchange multi-qubit entangled states simultaneously. Additionally, several enhanced QT schemes have been introduced, covering various communication scenarios, such as bidirectional quantum state sharing [19], bidirectional CQT [15, 20], cyclic QT [21, 22], and cyclic CQT [6, 23, 24], and so on.

Almost all of the above schemes involve the teleportation of a two-dimensional (2D) subspace of a quantum system, limiting quantum information to qubits only. However, in physics, quantum particles possess multiple degrees of freedom, allowing quantum systems to exist in higher-dimensional spaces. High-dimensional entanglement is an essential resource for quantum information processing. As a result, researchers have expanded QT to high-dimensional operations in both theoretical and practical contexts [25–27]. In [25], the teleportation of arbitrary high-dimensional quantum states in photonic systems is explored, providing an example of QT in a three-dimensional (3D) state. Additionally, [27] proposed bidirectional controlled teleportation scheme within a 3D quantum framework. In recent years, remarkable progress has been made in experimental implementations of high-dimensional QT. Hu *et al* [28] proposed and demonstrated a QT protocol based on spatial-mode entanglement for high-dimensional teleportation. Zhou *et al* [29] experimentally generated an asymmetric three-photon maximally entangled state and demonstrated its application potential in QT. Sephton *et al* realized stimulated teleportation of high-dimensional information using nonlinear spatial-mode detectors [30]. Moreover, recent works utilizing integrated photonic platforms and multiphoton interference systems have enabled scalable manipulation of high-dimensional entanglement. In 2025, a nonlinear high-dimensional QT protocol reported by Bianchi *et al* [31] further extended the technological boundaries of high-dimensional quantum communication. Clearly, compared with conventional 2D systems, high-dimensional QT schemes can transmit more quantum information and exhibit superior performance in specific applications. For instance, Brab and Macchiavello [32] demonstrated that qudit-based schemes for quantum cryptography offer greater security in noisy environments than those using qubit states. Furthermore, Klimov *et al* [33] emphasized that using qutrits for quantum computation significantly increases the available Hilbert space without requiring additional physical resources.

On the other hand, most existing studies on QT have neglected the influence of quantum noise. In realistic conditions, decoherence caused by the interaction between a quantum system and its environment can hardly be completely suppressed. Noise can attenuate the quantum state so that the received output state is inconsistent with the teleported state; therefore, it is crucial to investigate the impact of noise on QT schemes and to ascertain methods for enhancing the fidelity of the output state. In 2002, Oh *et al* [34] introduced noise into the study of QT schemes. They found that when the channel was affected by anisotropic noise, the fidelity of QT is lower than that of classical communication. However, when the noise was modeled using a Lindblad master equation, the teleportation fidelity remained above the classical threshold. Following this pioneering study, numerous quantum communication schemes operating under noisy environments have been proposed [35–43]. Researchers have systematically examined how different types of noise, such as amplitude damping, phase damping, and depolarizing processes, affect quantum communication by evaluating the corresponding fidelity, and a variety of noise-suppression techniques, including entanglement distillation and weak measurement, have been introduced to mitigate the detrimental effects of decoherence. To further improve the resilience of QT against realistic noise, several advanced schemes have been developed. Xiao *et al* [44] proposed a weak-measurement-based and environment-assisted protocol that significantly enhances teleportation performance under correlated amplitude-damping noise, effectively utilizing partial information about the environment to restore coherence. Dakir *et al* [45] explored the dynamical properties of QT in open two-qubit systems, revealing how quantum coherence and nonclassical correlations evolve under various noise regimes. Building upon these ideas, Kim and Jeong [46] investigated port-based entanglement teleportation using noisy resource states, offering a systematic framework to quantify entanglement degradation and suggesting a robust pathway for reliable state transfer in non-ideal quantum channels. Collectively, these studies reflect a transition from the passive mitigation of noise to actively exploiting environmental correlations and system-environment interactions to preserve quantum information, providing valuable insights for the development of more noise-tolerant teleportation protocols.

Most QT studies, however, are still predicated on the assumption that the quantum channel used to transmit entangled particles is memoryless, meaning that two consecutive uses of the channel are statistically independent. In practical scenarios, this assumption rarely holds, as residual correlations within the physical medium can give rise to memory effects that alter the dynamics of quantum information transfer. Macchiavello and Palma [47] were among the first to explore such effects by introducing a Pauli memory channel model, demonstrating that correlated noise can enhance the transmission of classical information in depolarizing channels. Subsequent research [48–51] has extended this concept to a variety of correlated noise environments, revealing that memory effects can fundamentally change the behavior and efficiency of quantum

communication processes. Recent studies have further deepened this understanding. D'Arrigo *et al* [48] demonstrated that correlations between successive uses of a Pauli noise channel can improve teleportation fidelity, while Zhang and Sun [51] proposed a remote-state-preparation protocol adapted to memory-enabled Pauli channels, quantitatively analyzing fidelity under five representative noisy models and showing that appropriate memory correlations can enhance communication efficiency. Xu *et al* [52] extended this analysis to high-dimensional QT systems, showing that Markovian memory can significantly improve robustness against environmental noise. Chen and Gong [53] further contributed by developing an efficient estimation method for Pauli channels with quantum mutual memory, enabling accurate characterization of correlated noise processes. Building on these advancements, Zhou [54] proposed an asymmetric cyclic CQT scheme under noisy conditions, illustrating how structured correlations among multiple entangled subsystems can maintain coherence and stabilize transmission performance. Taken together, these works demonstrate a clear evolution in the field, from treating noise as an unavoidable obstacle to recognizing it as a potentially exploitable resource. The growing body of research on memory-assisted and high-dimensional teleportation thus provides a strong theoretical foundation and motivation for exploring how memory correlations influence the fidelity of controlled QT in high-dimensional systems.

So far, there have been few studies on high-dimensional CQT in noisy channels with memory. Therefore, it is significant to study the effect of memory on the fidelity of high-dimensional CQT. In this paper, we investigate the realization of a CQT scheme for an arbitrary 3D single-qutrit state. Initially, we present the protocol in an ideal environment after constructing the tripartite qutrit entanglement channel. Subsequently, we analyze the propagation of 3D quantum states through four 3D-Pauli-like noisy channels with memory. In these channels, four types of 3D-Pauli-like disturbances corresponding to Weyl transformations are generated by Kraus operators: trit-flip, t-phase-flip, trit-phase-flip, and t-depolarizing. By allowing some of the qutrits to pass through the 3D-Pauli-like noisy channels with memory, we derive an analytic formula to quantify the average fidelity of the CQT scheme for each type of noisy channel. The findings indicate that the presence of memory in trit-flip and trit-phase-flip noise channels enhances the communication precision of CQT, whereas in t-phase-flip and t-depolarizing noisy channels, it diminishes the precision.

The arrangement of this paper is as follows. In section 2, we introduce the preliminaries relevant to the work, including descriptions of qutrits, the 3D-Bell state, Weyl operators, as well as measurement bases and unitary transformations for qutrits, and four types of 3D-Pauli-like disturbances characterized by Kraus operators. In section 3, the proposed scheme is described in an ideal environment. In section 4, the scheme is presented in each of the four types of 3D-Pauli-like noisy channels with memory, and the relationship between fidelity, memory, and noise parameters is identified. We conclude the paper in section 5.

2. Preliminaries

In this section, we introduce fundamental concepts essential to the work, including qutrits, 3D-Bell states, 3D-GHZ states, unitary transformations for qutrits, Weyl operators, and 3D-Pauli-like noise.

2.1. Qutrit, 3D-Bell state and 3D-GHZ state

Similar to the classical trit, the basic unit of information in a 3D quantum system is known as a qutrit. A qutrit exists as a superposition of the computational basis states $|0\rangle$, $|1\rangle$ and $|2\rangle$, and can be generally expressed as

$$|\varphi\rangle = \alpha|0\rangle + \beta|1\rangle + \gamma|2\rangle, \tag{1}$$

where α, β and γ are complex numbers satisfying the normalization condition $|\alpha|^2 + |\beta|^2 + |\gamma|^2 = 1$. In specific cases, it can also be derived from [43] as follows

$$\begin{aligned}|\varphi\rangle = \cos\frac{\theta}{2}|0\rangle + \sin\frac{\theta}{2}\cos\frac{\tau}{2}e^{i\vartheta}|1\rangle \\ + \sin\frac{\theta}{2}\cos\frac{\tau}{2}e^{i\vartheta'}|2\rangle,\end{aligned} \tag{2}$$

here $\theta, \tau \in [0, \pi]$ and $\vartheta, \vartheta' \in [0, 2\pi]$, and the symbol i denotes the imaginary unit satisfying $i = \sqrt{-1}$. The general form of a two-particle Bell state in a high-dimensional quantum system can be represented as [55]

$$|\phi_{st}\rangle = \frac{1}{\sqrt{d}}\sum_{j=0}^{d-1} e^{2\pi ijs/d}|j\rangle \otimes |(j+t) \bmod d\rangle, \tag{3}$$

where $s, t = 0, 1, 2, \cdots, d-1$. When $d = 3$, the nine 3D-Bell states are given by:

$$\begin{aligned}|\phi_{00}\rangle &= \frac{1}{\sqrt{3}}(|00\rangle + |11\rangle + |22\rangle) \\ |\phi_{10}\rangle &= \frac{1}{\sqrt{3}}(|00\rangle + e^{2\pi i/3}|11\rangle + e^{4\pi i/3}|22\rangle) \\ |\phi_{20}\rangle &= \frac{1}{\sqrt{3}}(|00\rangle + e^{4\pi i/3}|11\rangle + e^{2\pi i/3}|22\rangle) \\ |\phi_{01}\rangle &= \frac{1}{\sqrt{3}}(|01\rangle + |12\rangle + |20\rangle) \\ |\phi_{11}\rangle &= \frac{1}{\sqrt{3}}(|01\rangle + e^{2\pi i/3}|12\rangle + e^{4\pi i/3}|20\rangle) \\ |\phi_{21}\rangle &= \frac{1}{\sqrt{3}}\left(|01\rangle + e^{4\pi i/3}|12\rangle + e^{2\pi i/3}|20\rangle\right)\end{aligned}$$

$$|\phi_{02}\rangle = \frac{1}{\sqrt{3}}(|02\rangle + |10\rangle + |21\rangle)$$
$$|\phi_{12}\rangle = \frac{1}{\sqrt{3}}\left(|02\rangle + e^{2\pi i/3}|10\rangle + e^{4\pi i/3}|21\rangle\right)$$
$$|\phi_{22}\rangle = \frac{1}{\sqrt{3}}\left(|02\rangle + e^{4\pi i/3}|10\rangle + e^{2\pi i/3}|21\rangle\right). \quad (4)$$

By using an additional single photon, the nine 3D-Bell stateshave been shown to be distinguishable, which is described in detail in [25]. Therefore, they can form a basis $\{|\phi_{st}\}$ for jointly measuring two-qutrit states. An n-particle d-dimensional entangled quantum state can be expressed as [56, 57]:

$$|\phi(u_1, u_2, \cdots, u_n)\rangle = \frac{1}{\sqrt{d}}\sum_{j=0}^{d-1} e^{2\pi i j u_1/d}|j, j+u_2, \cdots, j+u_n\rangle. \quad (5)$$

When $n=3, d=3$ and $u_j = 0$ $(j=1,2,3)$, the 3D-GHZ state can be written as

$$|\mathcal{G}\rangle = \frac{1}{\sqrt{3}}(|000\rangle + |111\rangle + |222\rangle. \quad (6)$$

2.2. 3D measurement bases, 3D unitary operations and Weyl operators

In order to realize the transmission of the qutrit states, we need to introduce some basic measurement bases and unitary operations. Similar to the Z-basis and X-basis, which are often used for measurement in 2D quantum systems, the measurement bases for the 3D quantum system are defined as [34]:

$$3D-Z-basis: \{|0\rangle, |1\rangle, |2\rangle\},$$
$$3D-X-basis: \left\{|\mathcal{X}_j\rangle = \frac{1}{\sqrt{3}}\sum_{k=0}^{2} e^{2\pi ijk}|k\rangle | j=0,1,2\right\}. \quad (7)$$

In a 2D quantum system, the Hadamard transform can convert the computation basis states $|0\rangle$ and $|1\rangle$ to the superposition states $|+\rangle = \frac{1}{\sqrt{2}}(|0\rangle + |1\rangle)$ and $|-\rangle = \frac{1}{\sqrt{2}}(|0\rangle - |1\rangle)$, respectively. The corresponding transform $H^{(3)}$ in a 3D quantum system can be expressed as in [34, 57]

$$H^{(3)} = \frac{1}{\sqrt{3}}\sum_{j,l=0}^{2} e^{2\pi i/3}|j\rangle\langle l| = \frac{1}{\sqrt{3}}\begin{pmatrix} 1 & 1 & 1 \\ 1 & e^{2\pi i/3} & e^{4\pi i/3} \\ 1 & e^{4\pi i/3} & e^{2\pi i/3} \end{pmatrix}. \quad (8)$$

A 3D-controlled NOT gate $\mathcal{C}_{ij}^{(3)}$ in a 3D quantum system is defined as [34]:

$$\mathcal{C}_{ij}^{(3)}|s\rangle_i|t\rangle_j = |s\rangle_i|(s+t)\,\mathrm{mod}3\rangle_j, \quad (9)$$

where i denotes the controlled qutrit, and j represents the target qutrit. Weyl operators in a d-dimensional quantum system, analogous to Pauli operators in 2D quantum systems, serve as transformations for high-dimensional states, and can be expressed as [34]:

$$(U_{kl})_{j'j} = e^{2\pi ijk/d}\delta_{j',(j+l)\mathrm{mod}d}, \quad (10)$$

where $k, l, j', j = 0, 1, \cdots, d-1$.

2.3. 3D-Pauli-like noise

Quantum noise is an inevitable phenomenon in physical QT, resulting in the received output state diverging from the transmitted state due to the effects of decoherence. In 2D quantum systems, the most common type of noise is Pauli noise, which includes bit-flip, phase-flip, bit-phase-flip, and depolarizing noise, each determined by different Pauli operators.

Within a 3D quantum system, the corresponding Pauli noise, termed 3D-Pauli-like noise, encompasses trit-flip noise, t-phase-flip noise, trit-phase-flip noise, and t-depolarizing noise, respectively. These types of noise depend on the Weyl operator and are briefly described using Kraus operators [34]. Here, p represents the noise strength, that is, the probability that the quantum state is affected by the 3D-Pauli-like noise within the quantum channel. Its value lies within the range $0 \leqslant p \leqslant 1$. When $p=0$, the channel is ideal and noiseless; when $p=1$, the channel is completely disturbed by noise.

The Kraus operators corresponding to trit-flip noise are given by

$$E_{00} = \sqrt{1-p}U_{00},\ E_{01} = \sqrt{p/2}U_{01},\ E_{02} = \sqrt{p/2}U_{02}, \quad (11)$$

where p denotes the probability of a flip.

The Kraus operators corresponding to t-phase-flip noise are

$$E_{00} = \sqrt{1-p}U_{00},\ E_{10} = \sqrt{p/2}U_{10},\ E_{20} = \sqrt{p/2}U_{20}, \quad (12)$$

where p denotes the probability of a phase shift.

The Kraus operators corresponding to trit-phase-flip noise are

$$E_{00} = \sqrt{1-p}U_{00},\ E_{11} = \sqrt{p/2}U_{11},\ E_{12} = \sqrt{p/2}U_{12},$$
$$E_{21} = \sqrt{p/2}U_{21},\ E_{22} = \sqrt{p/2}U_{22}, \quad (13)$$

where p denotes the probability of a phase shift.

The Kraus operators corresponding to t-depolarizing noise are

$$E_{00} = \sqrt{1-\frac{8}{9}p}U_{00},\ E_{01} = \frac{\sqrt{p}}{3}U_{01},\ E_{02} = \frac{\sqrt{p}}{3}U_{02},$$
$$E_{10} = \frac{\sqrt{p}}{3}U_{10},\ E_{11} = \frac{\sqrt{p}}{3}U_{11},\ E_{12} = \frac{\sqrt{p}}{3}U_{12},$$
$$E_{20} = \frac{\sqrt{p}}{3}U_{20},\ E_{21} = \frac{\sqrt{p}}{3}U_{21},\ E_{22} = \frac{\sqrt{p}}{3}U_{22}, \quad (14)$$

where p denotes the depolarization probability.

3. Deterministic controlled teleportation of an unknown single-qutrit state

In this section, we provide a comprehensive description of a 3D CQT scheme designed for transmitting an unknown single-qutrit state in an ideal environment. The protocol involves three parties situated at distinct locations: two observers, Alice and Bob, and a controller, Charlie. Assuming Alice wishes to send an arbitrary unknown single-qutrit state $|\xi\rangle_A$ to Bob, this state can be expressed as

$$|\xi\rangle_A = a_0|0\rangle + a_1|1\rangle + a_2|2\rangle, \tag{15}$$

where a_0, a_1 and a_2 are complex numbers that satisfy $|a_0|^2 + |a_1|^2 + |a_2|^2 = 1$. Bob can successfully receive the state only when the communication is permitted by the controller, Charlie.

The CQT procedure consists of the following four steps.

Step 1 Charlie needs to prepare a three-qutrit entangled state in a 3D quantum system as follows

$$\begin{aligned}|\mathcal{Q}\rangle = \frac{1}{3}[&|0\rangle_1(|00\rangle + |11\rangle + |22\rangle)_{23} \\ &+ |1\rangle_1(|00\rangle + e^{2\pi i/3}|11\rangle + e^{4\pi i/3}|22\rangle)_{23} \\ &+ |2\rangle_1(|00\rangle + e^{4\pi i/3}|11\rangle + e^{2\pi i/3}|22\rangle)_{23}].\end{aligned} \tag{16}$$

The specific preparation process is as follows: the input state is the three-qutrit product state $|\psi_1\rangle = |0\rangle_1|0\rangle_2|0\rangle_3$. Applying the first Hadamard operation $H^{(3)}$ to particle 1, we obtain the state

$$|\psi_2\rangle = H^{(3)}|\psi_1\rangle = \frac{1}{\sqrt{3}}(|000\rangle + |100\rangle + |200\rangle)_{123}. \tag{17}$$

Subsequently, Charlie performs a controlled-NOT operation $\mathcal{C}_{ij}^{(3)}$ on the particle pair $(1,2)$, with qubit 1 acting as the controlled particle and qubit 2 as the target. This operation transforms the state $|\psi_2\rangle$ into

$$|\psi_3\rangle = \mathcal{C}_{12}^{(3)}|\psi_2\rangle = \frac{1}{\sqrt{3}}(|000\rangle + |110\rangle + |220\rangle)_{123}. \tag{18}$$

Next, particle 2 is sent through a Hadamard operation, then the state $|\psi_3\rangle$ can be transformed into

$$\begin{aligned}|\psi_4\rangle = \frac{1}{3}[&|0\rangle_1(|00\rangle + |10\rangle + |20\rangle)_{23} \\ &+ |1\rangle_1(|00\rangle + e^{2\pi i/3}|10\rangle + e^{4\pi i/3}|20\rangle)_{23} \\ &+ |2\rangle_1(|00\rangle + e^{4\pi i/3}|10\rangle + e^{2\pi i/3}|20\rangle)_{23}].\end{aligned} \tag{19}$$

Finally, a 3D controlled-NOT operation is applied to particles $(2,3)$. The state $|\psi_4\rangle$ then evolves into

$$\begin{aligned}|\psi_5\rangle &= \mathcal{C}_{23}^{(3)}|\psi_4\rangle \\ &= \frac{1}{3}[|0\rangle_1(|00\rangle + |11\rangle + |22\rangle)_{23} \\ &\quad + |1\rangle_1(|00\rangle + e^{2\pi i/3}|11\rangle + e^{4\pi i/3}|22\rangle)_{23} \\ &\quad + |2\rangle_1(|00\rangle + e^{4\pi i/3}|11\rangle + e^{2\pi i/3}|22\rangle)_{23}].\end{aligned} \tag{20}$$

Obviously, $|\psi_5\rangle = |\mathcal{Q}\rangle$.

After obtaining the quantum state $|\mathcal{Q}\rangle$, Charlie needs to send qutrits 2 and 3 to Alice and Bob, respectively, and keep qutrit 1 for himself.

The state of the entire quantum system, comprising the teleported state $|\xi\rangle_A$ and the channel $|\mathcal{Q}\rangle$, is represented as

$$|T\rangle = |\xi\rangle_A \otimes |\mathcal{Q}\rangle. \tag{21}$$

Step 2 Alice performs a joint measurement on the qutrit pair $(2,A)$ in the 3D-Bell basis and records her measurement outcome. She then transmits the corresponding classical information to Bob through a classical channel.

Utilizing a 3D-Bell basis

$$\left\{|\phi_{mn}\rangle = \frac{1}{\sqrt{3}}\sum_{j=0}^{2} e^{2\pi ijm/3}|j\rangle \otimes |(j+n)\bmod 3\rangle | m,n = 0,1,2\right\}, \tag{22}$$

the state of the initial system presented in equation (21) can be represented as

$$|T\rangle = \frac{1}{3\sqrt{3}}\sum_{r=0}^{2}\sum_{m,n=0}^{2}|\phi_{mn}\rangle_{2A}|r\rangle_1\left[\sum_{k=0}^{2} a_{(k+n)\bmod 3} e^{2\pi ik(r-m)/3}|k\rangle_3\right]. \tag{23}$$

Generally, if Alice's measurement result is $|\phi_{mn}\rangle_{2A}$, then the state of the remaining particles will be collapsed into

$$|\dot{T}\rangle = \frac{1}{3\sqrt{3}}\sum_{r=0}^{2}|r\rangle_1\left[\sum_{k=0}^{2}a_{(k+n)\bmod 3}e^{2\pi ik(r-m)/3}|k\rangle_3\right]. \tag{24}$$

Step 3 If Charlie permits the communication between Alice and Bob, he must perform a single-qutrit measurement in the 3D-Z-basis on qutrit 1. The measurement outcome will correspond to one of the states $|r\rangle_1$ where $r=0,1,2$, each occurring with an equal probability of $1/3$. Following this measurement, the state of qutrit 3 will be transformed into

$$|\ddot{T}\rangle = {}_1\langle r|\dot{T}\rangle = \frac{1}{3}\left[\sum_{k=0}^{2}a_{(k+n)\bmod 3}e^{2\pi ik(r-m)/3}|k\rangle_3\right]. \tag{25}$$

Following the measurement, Charlie must convey his measurement outcome to Bob using classical communication.

Step 4 After receiving the measurement results from Alice and Charlie, Bob needs to perform preform a unitary transformation

$$U_B = |n\rangle\langle 0| + e^{2\pi i(m-r)/3}|(n+1)\bmod 3\rangle \times\langle 1| + e^{4\pi i(m-r)/3}|(n+2)\bmod 3\rangle\langle 2|$$

on qutrit 3 to reconstruct the desired state $|\xi\rangle_A$.

It is straightforward to verify that U_B is a Weyl operator in 3D quantum systems for any $r,m,n\in\{0,1,2\}$. Clearly, there are 9×3 such collapse states in equation (25), each occurring with a probability of $1/9\times 1/3$. Following the aforementioned four steps, Bob can consistently reconstruct the desired quantum state $|\xi\rangle_A$ by applying the appropriate 3D Weyl operator, resulting in a total success probability of

$$\left(\frac{1}{9}\times\frac{1}{3}\right)\times 27 = 1.$$

4. Controlled teleportation in 3D-Pauli-like noisy channels with memory

It is well-recognized that communication environments in the real world are not devoid of noise. Thus,in order to construct a practical quantum communication scheme, it is essential to understand and control the quantum noise process. Naturally, an important question arises: how does noise in the quantum channel affect the procedure of controlled QT (CQT) in a 3D system? In this segment, we investigate how quantum noise influences the process of CQT within a 3D system, maintaining the assumption that the 3D entangled state $|\mathcal{Q}\rangle$, as outlined in equation (16), serves as the quantum channel initially prepared by Charlie. In this setup, Charlie retains qutrit 1 while sending qutrit 2 to Alice and qutrit 3 to Bob through their respective quantum communication channels. Suppose that during transmissions, qutrits 2 and 3 experience 3D-Pauli-like noise. The evolution of the entangled channel $|\mathcal{Q}\rangle$ under the effect of 3D-Pauli-like noise can be represented by the density operator as follows:

$$\rho_{en} = \sum_{m,n,k,l=0}^{2} p_{mn,kl}U_{00}\otimes U_{mn}\otimes U_{kl}|\mathcal{Q}\rangle\langle\mathcal{Q}|\left(U_{00}\otimes U_{mn}\otimes U_{kl}\right)^{\dagger},$$
$$p_{mn,kl} = p_{mn}p_{kl}, \tag{26}$$

where the noise parameters p_{mn} and p_{kl} correspond to the probabilities associated with the operators U_{mn} and U_{kl} acting on qutrits 2 and 3, respectively. However, in practical communication scenarios, when qutrits 2 and 3 are transmitted through a noisy channel with minimal temporal separation, a degree of correlation arises between the two uses of the channel. In this study, we propose that the correlation exhibits Markovian properties, which can be described by

$$p_{mn,kl} = (1-\mu)\,p_{mn}p_{kl} + \mu p_{mn}\delta_{mn,kl}, \tag{27}$$

where $\delta_{mn,kl}=1$ when $mn=kl$ and $\delta_{mn,kl}=0$ when $mn\neq kl$. The parameter μ $(0\leqslant\mu\leqslant 1)$ represents the memory coefficient of the quantum channel, characterizing the degree of correlation between consecutive channel uses. Specifically, when $\mu=0$, the channel is memoryless, and each noise event occurs independently; whereas when $\mu=1$, the channel is fully

correlated, meaning that the same noise acts identically on both transmitted qutrits.

Based on equation (27), the density operator ρ_{en} can be reformulated as

$$\begin{aligned}\rho_{en} = &\sum_{m,n,k,l=0}^{2} \left[(1-\mu)\,p_{mn}p_{kl} + \mu p_{mn}\delta_{mn,kl}\right] U_{00}\otimes U_{mn}\otimes U_{kl}|\mathcal{Q}\rangle \times \langle\mathcal{Q}|\,(U_{00}\otimes U_{mn}\otimes U_{kl})^{\dagger} \\ = &(1-\mu)\sum_{m,n,k,l=0}^{2} p_{mn}p_{kl}U_{00}\otimes U_{mn}\otimes U_{kl}|\mathcal{Q}\rangle\langle\mathcal{Q}|\,(U_{00}\otimes U_{mn}\otimes U_{kl})^{\dagger} \\ &+\mu\sum_{m,n=0}^{2} p_{mn}U_{00}\otimes U_{mn}\otimes U_{mn}|\mathcal{Q}\rangle\langle\mathcal{Q}|\,(U_{00}\otimes U_{mn}\otimes U_{mn})^{\dagger}. \end{aligned} \tag{28}$$

By implementing the CQT described in section 3 through the channel ρ_{en}, and performing the subsequent measurement operations and unitary transformations, Bob can obtain the output state represented by the density operator

$$\begin{aligned}\rho_{\text{out}}^{mnr} = U_B \text{tr}_{2,A,1}\{&|r\rangle_1\langle r|\otimes|\phi_{mn}\rangle_{2A}\langle\phi_{mn}||\xi\rangle_A\langle\xi| \\ &\otimes\rho_{en}(|\phi_{mn}\rangle_{2A}\langle\phi_{mn}|)^{\dagger}\otimes(|r\rangle_1\langle r|)^{\dagger}\}(U_B)^{\dagger},\end{aligned} \tag{29}$$

where $\text{tr}_{2,A,1}$ denotes the partial trace over qutrits $2, A$, and 1. In a perfect teleportation scenario, the output density operator ρ_{out}^{mnr} will match the density $|\xi\rangle_A\langle\xi|$ of the teleported state, aside from a normalization factor. However, in the presence of quantum noise, there will be a divergence between the two density operators. The fidelity of the teleportation process, which quantifies how closely the output state ρ_{out}^{mnr} approximates the desired teleported state, can be determined by

$$F^{mnr} = \langle\xi|\rho_{\text{out}}^{mnr}|\xi\rangle. \tag{30}$$

Mean fidelity is defined in terms of all possible measurement results as

$$F_{av} = \sum_{m,n,r=0}^{2} p_{nmr}F^{mnr}, \tag{31}$$

where p_{mnr} depends on the coefficients of the teleported state ρ_{out}^{mnr}.F_{av} primarily depends on the coefficients of the teleported state $|\xi\rangle_A$ and thus, it is more practical to compute the average fidelity over the ensemble of input states [35, 55]

$$\langle F\rangle = \frac{2}{\pi^2}\int_0^{\pi}\int_0^{\pi}\int_0^{2\pi}\int_0^{2\pi}\sin^3\frac{\theta}{2}\sin\frac{\tau}{2}\cos\frac{\theta}{2}\cos\frac{\tau}{2}\text{d}\theta\text{d}\tau\text{d}\vartheta\text{d}\vartheta' F_{av} \tag{32}$$

by using the following relationships $a_0 = \cos\frac{\theta}{2}, a_1 = \sin\frac{\theta}{2}\cos\frac{\tau}{2}e^{i\vartheta}$ and $a_2 = \sin\frac{\theta}{2}\sin\frac{\tau}{2}e^{i\vartheta'}$ of state $|\xi\rangle_A$ in accordance to equation (2).

4.1. Calculation of the fidelities

In this subsection, we consider the average fidelity of the 3D-CQT scheme for four types of 3D-Pauli-like noise in channels with memory. By using the Kraus operators for the four types of 3D-Pauli-like noise, the channel noise for each type in a memory-inclusive channel can be obtained by setting different noise parameters p_{mn} $(m, n = 0, 1, 2)$ in equation (28), specifically.

The trit-flip channel with memory can be given by $p_{00} = 1-p, p_{01} = p_{02} = p/2$, and $p_{10} = p_{11} = p_{12} = p_{20} = p_{21} = p_{22} = 0$.

The t-phase-flip channel with memory is characterized by $p_{00} = 1-p, p_{10} = p_{20} = p/2$, and $p_{01} = p_{02} = p_{11} = p_{12} = p_{21} = p_{22} = 0$.

The trit-phase-flip noise in a memory-inclusive channel can be obtained by setting $p_{00} = 1-p, p_{11} = p_{12} = p_{21} = p_{22} = p/4$ and $p_{01} = p_{02} = p_{10} = p_{20} = 0$.

The trit-phase-flip disturbance in a memory-inclusive channel is given by setting noise parameters $p_{00} = 1-8p/9$ and $p_{01} = p_{02} = p_{10} = p_{20} = p_{11} = p_{12} = p_{21} = p_{22} = p/9$. For these specific noise channels, the average fidelity can be calculated by following the steps outlined below.

Firstly, based on the equation $\int\int\int\int \sin^3\frac{\theta}{2}\sin\frac{\tau}{2}\cos\frac{\theta}{2}\cos\frac{\tau}{2}\mathrm{d}\theta\mathrm{d}\tau\mathrm{d}\vartheta\mathrm{d}\vartheta' = \int \mathrm{d}\Gamma_3$ (see [58]), equation (32) can then be expressed as

$$\langle F\rangle = \frac{2}{\pi^2}\int \mathrm{d}\Gamma_3 F_{av}. \tag{33}$$

Second, the expression of F_{av} consists of a_0, a_1, a_2, p and u. Therefore, the integral over F_{av} can be regarded as the integral over a_0, a_1 and a_2. Then, combining this with the equation from [58]

$$\frac{2}{\pi^2}\int \mathrm{d}\Gamma_3 a_j a_k^* a_l a_m^* = \frac{1}{12}\left(\delta_{jk}\delta_{lm}+\delta_{jm}\delta_{kl}\right), \tag{34}$$

the following equation holds

$$\begin{aligned}\int \mathrm{d}\Gamma_3|a_0|^4 &= \int \mathrm{d}\Gamma_3|a_1|^4 = \int \mathrm{d}\Gamma_3|a_2|^4 = \frac{\pi^2}{12},\\ \int \mathrm{d}\Gamma_3|a_0|^2|a_1|^2 &= \int \mathrm{d}\Gamma_3|a_0|^2|a_2|^2\\ &= \int \mathrm{d}\Gamma_3|a_1|^2|a_2|^2 = \frac{\pi^2}{24}.\end{aligned} \tag{35}$$

Finally, the average fidelity can be obtained by substituting equation (35) into equation (33). Therefore, the average fidelity under these four types noise channels with memory can be expressed as

$$\begin{aligned}\langle F\rangle_F &= 1-\frac{3}{2}p+\frac{9}{8}p^2+\frac{3}{2}p\mu\left(1-\frac{3}{4}p\right),\\ \langle F\rangle_P &= 1-\frac{3}{2}p+\frac{9}{8}p^2+\frac{3}{4}p\mu\left(1-\frac{3}{2}p\right),\\ \langle F\rangle_{FP} &= 1-\frac{3}{2}p+\frac{15}{16}p^2+\frac{3}{4}p\mu\left(1-\frac{5}{4}p\right),\\ \langle F\rangle_D &= 1-\frac{4}{3}p+\frac{2}{3}p^2+\frac{1}{6}p\mu(5-4p).\end{aligned} \tag{36}$$

for $0\leqslant p,\mu\leqslant 1$, where $\langle F\rangle_F$ is the average fidelity of the trit-flip noise channel, $\langle F\rangle_P$ is the average fidelity for the t-phase-flip noise, $\langle F\rangle_{FP}$ is the average fidelity for the trit-phase-flip noise, and $\langle F\rangle_D$ is the average fidelity for the t-depolarizing noise with memory, respectively.

4.2. Analysis of the effect of memory on the average fidelity

Now, we analyze the effect of memory on the average fidelity for each type of noise channel. From equation (36), the partial derivatives of the average fidelities with respect to the memory parameter for the four noise channels are given by

$$\begin{aligned}\frac{\partial\langle F\rangle_F}{\partial\mu} &= \frac{1}{2}p\left(1-\frac{3}{4}p\right)\geqslant 0.\\ \frac{\partial\langle F\rangle_P}{\partial\mu} &= \frac{3}{4}p\left(1-\frac{3}{2}p\right) = \begin{cases}>0, & 0<p<2/3;\\ \leqslant 0, & p=0\ or\ 2/3\leqslant p\leqslant 1.\end{cases}\\ \frac{\partial\langle F\rangle_{FP}}{\partial\mu} &= \frac{3}{4}p\left(1-\frac{5}{4}p\right) = \begin{cases}>0, & 0<p<4/5;\\ \leqslant 0, & p=0\ or\ 4/5\leqslant p\leqslant 1.\end{cases}\\ \frac{\partial\langle F\rangle_D}{\partial\mu} &= \frac{1}{6}p(5-4p)\geqslant 0.\end{aligned} \tag{37}$$

Equation (37) indicates that average fidelities $\langle F\rangle_F$ and $\langle F\rangle_D$ increase as the memory parameter μ increases, independent of the noise parameter p. However, for average fidelities $\langle F\rangle_P$ and $\langle F\rangle_{FP}$, we observe respective threshold values ($p=2/3$ and $p=4/5$) derived from equation (37). $\langle F\rangle_P$ and $\langle F\rangle_{FP}$ increase as the memory parameter increases only when the noise intensity p is below the corresponding threshold value. In other words, for trit-flip noise and t-depolarizing noise, the fidelity of controlled teleportation can be improved by increasing the value of channel memory, even for the strongest noise. However, for t-phase-flip noise and trit-phase-flip noise, the controlled teleportation accuracy can only be improved by increasing the value of channel memory if the noise intensity p satisfies a certain condition (i.e. p must not exceed the corresponding threshold). Figure 1 illustrates the relationship between the average fidelity and the memory parameter for the three scenarios $p=0.1, 0.5, 0.9$, as specified in equation (36).

Figure 1 illustrates that, for all three values of p, the average fidelities $\langle F\rangle_F$ and $\langle F\rangle_D$ increase with an increase in the memory parameter. In contrast, the average fidelities $\langle F\rangle_P$ and $\langle F\rangle_{FP}$ initially decrease as μ increases in panel (a) and (b), and continue to decrease with μ in panel (c).

Specifically, when $p=0.1$, $\langle F\rangle_F$ and $\langle F\rangle_D$ increased from 0.861 and 0.873 to 1 and 0.95 respectively, while $\langle F\rangle_P$ and $\langle F\rangle_{FP}$ decrease from 0.861 and 0.859 to 0.925 and 0.925 respectively.

When $p=0.5$, $\langle F\rangle_F$ and $\langle F\rangle_D$ increased from 0.531 and 0.5 to 1 and 0.75 respectively, while $\langle F\rangle_P$ and $\langle F\rangle_{FP}$ increased from 0.531 and 0.484 to 0.625 and 0.625 respectively.

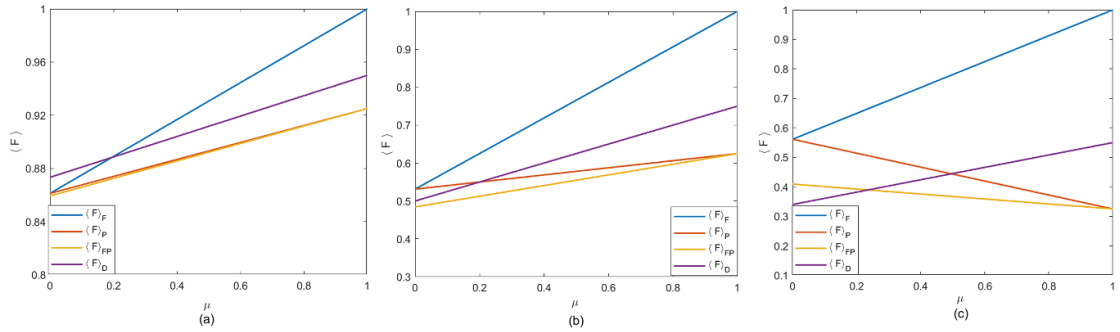

Figure 1. The relation between μ and $\langle F\rangle$, where $p=0.1$ in (a) $p=0.5$ in (b) $p=0.9$ in (c).

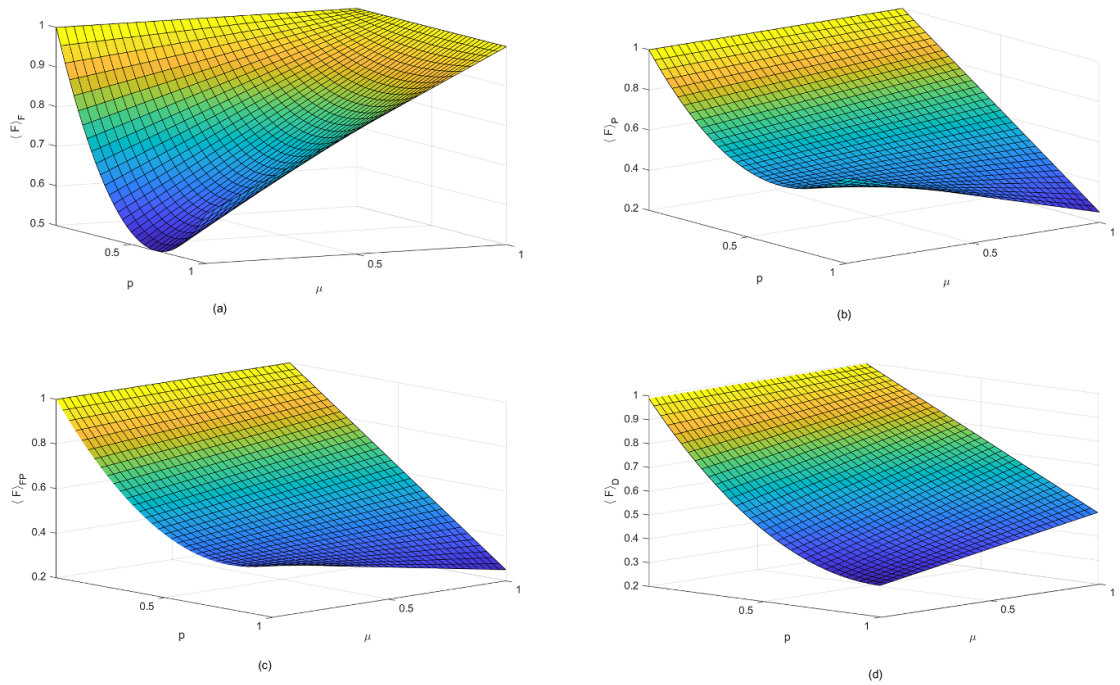

Figure 2. The effect of the noise parameter p and the memory parameter μ on the average fidelity for the four types of noise.

When $p=0.9$, $\langle F\rangle_F$ and $\langle F\rangle_D$ increased from 0.561 and 0.34 to 1 and 0.55 respectively, while $\langle F\rangle_P$ and $\langle F\rangle_{FP}$ decreased from 0.561 and 0.409 to 0.325 and 0.325, respectively.

The combined of the noise parameter p and the memory parameter μ on the average fidelities for the four types of noise channels is shown in figure 2.

It can be roughly observed from figure 2 that for trit-flip and t-depolarizing noise channels, memory helps to slow down the degradation of the average fidelity due to noise, thus improving the accuracy of CQT. However, for t-phase-flip and trit-phase-flip channel noise channels, each type of noise has a specific threshold intensity, denoted as p^*. Below this threshold, increasing memory improves the average fidelity. Beyond this threshold, however, increasing memory results in a decrease in average fidelity.

Furthermore, by examining figure 2 in detail, we can draw the following conclusions:

(a) Trit-flip noise

When $\mu=0$, i.e. it is irrelevant that Alice and Bob continue to use the channel, the average fidelity $\langle F\rangle_F$ satisfies $\langle F\rangle_F=\frac{1}{2}+\frac{9}{8}(p-\frac{2}{3})^2$, which attains its minimum 1/2 at $p=2/3$, and reaches its maximum value of 1 at $p=0$. Figure 2(a) shows that when $\mu=0$, the average fidelity $\langle F\rangle_F$ initially decreases from 1 and then increases as the noise parameter p increase , reaching its minimum value of $1/2$ when $p\approx 0.7$. However, when $\mu>0$ (i.e. the channel has memory), $\langle F\rangle_F$ is always greater than $1/2$, and it increases as μ increases. When $\mu=1$, $\langle F\rangle_F$ is always at its maximum value of 1, regardless of p. This observation confirms that memory in trit-flip noisy channel improves the

efficiency of the controlled teleportation scheme and that the scheme becomes immune to trit-flip noise when there is a strong correlation between two successive uses of the channel.

(b) Trit-phase-flip noise
When $\mu = 0$, the average fidelity is given by $\langle F\rangle_{FP} = \frac{2}{5} + \frac{15}{16}(p - \frac{4}{5})^2$, which attains its minimum 2/5 at $p = 4/5$, and reaches its maximum 1 at $p = 0$. Figure 2(b) shows that when $\mu = 0$, $\langle F\rangle_{FP}$ initially decreases and then increases with the increase of the noise parameter p, reaching its minimum value of 0.4 when $p = 0.8$. When $\mu > 0$, $\langle F\rangle_{FP}$ is always no less than 0.25, and from figure 2(b), there is a region where $\langle F\rangle_{FP}$ is less than $1/2$. This region does not change significantly as the memory parameters increase. That is, an increase in memory does not increase resistance to this type of noise as it does to the trit-flip noise.

When $\mu = 1$, the average fidelity $\langle F\rangle_{FP}$ decreases in a straight line and reaches the minimum value of 0.25 when $p = 1$. That means that when Alice and Bob's continued use of the channel is completely relevant, the maximum reduction in the average fidelity $\langle F\rangle_{FP}$ occurs by increasing the noise parameter, compared with other memory values.

(c) T-phase-flip noise
When $\mu = 0$, the average fidelity $\langle F\rangle_P$ is given by $\langle F\rangle_P = \frac{1}{2} + \frac{9}{8}(p - \frac{2}{3})^2$, similar to $\langle F\rangle_F$, $\langle F\rangle_P$ attains its minimum value of $1/2$ at $p = 2/3$ and reaches its maximum value of 1 at $p = 0$. Figure 2(c) shows that when $\mu = 0$, the average fidelity $\langle F\rangle_P$ initially decreases and then increases as the noise parameter p increase, reaching its minimum value of $1/2$ when $p \approx 0.7$. Like $\langle F\rangle_{FP}$, when $\mu > 0$, $\langle F\rangle_P$ is always no less than 0.25, and there is also a region where $\langle F\rangle_P$ is less than $1/2$, which does not change significantly as the memory parameters increase. This shows that an increase in memory does not increase resistance to this type of noise as it does to the trit-flip noise. When $\mu = 1$, $\langle F\rangle_p$ drops from 1 to 0.25 in a straight line as the noise parameter increases from 0 to 1, i.e. This observation confirms that maximum memory in the t-phase-flip noisy channel greatly promotes the decline of CQT efficiency.

(d) T-depolarizing noise
When $\mu = 0$, the average fidelity $\langle F\rangle_D$ is expressed as $\langle F\rangle_D = \frac{1}{3} + \frac{2}{3}(p_1)^2$, which reaches its minimum value of $1/3$ at $p = 1$, and attains its maximum value of 1 at $p = 0$. Figure 2(d) shows that when $\mu = 0$, the average fidelity $\langle F\rangle_D$ always decreases as the noise parameter p increases, reaching the minimum value of $1/3$ when $p = 1$. However, when $\mu > 0$, $\langle F\rangle_D$ is always greater than $1/3$, and it increases as μ increases. When $\mu = 1$, $\langle F\rangle_D$ is not always less than 1/2. This observation confirms that memory in a t-depolarizing noisy channel increases the robustness of the scheme, i.e. regardless of the noise intensity, increasing the memory parameter in the t-depolarizing noise channel can always improve the precision of CQT.

5. Conclusion

By employing 3D-Hadamard gates and 3D-controlled NOT gates, this paper constructs a three-qutrit maximally entangled state in a 3D quantum system and subsequently proposes a 3D CQT scheme in an ideal environment. In this scheme, Alice, under Charlie's control, successfully transmits an arbitrary unknown single-qutrit state to Bob with a 100% success probability, using the three-qutrit entangled state constructed in this work as the quantum channel.

To further evaluate the robustness of this CQT scheme, fidelity is employed to quantify its performance in a 3D Pauli-like noisy environment. Four typical types of 3D Pauli noise-trit-flip, trit-phase-flip, t-phase-flip, and t-depolarizing noise-are analyzed. The model assumes that the qutrits of both sender and receiver pass through their respective noisy channels consecutively, with only a short time interval between them. Due to this temporal proximity, the two channel uses are correlated, and the channel can thus be regarded as a memory channel. In this study, we derive the analytical relationships between the average fidelity of the CQT process and the noise parameters for the four types of 3D Pauli-like noisy channels with memory. Furthermore, we obtain the partial derivatives of the average fidelity with respect to the memory parameter for each noise type. The results indicate that these partial derivatives are positive for trit-flip and t-depolarizing noise channels, implying that increasing memory enhances teleportation fidelity. In contrast, for t-phase-flip and trit-phase-flip noise channels, a threshold behavior is observed: when the noise parameter exceeds a specific value, the partial derivative becomes negative, meaning that memory effects deteriorate teleportation fidelity beyond this threshold.

In summary, this work proposes a novel 3D CQT scheme for an arbitrary unknown single-qutrit state using a newly constructed three-qutrit maximally entangled channel. Under realistic 3D Pauli-like noisy environments, our analysis reveals that memory effects can enhance the performance of CQT in trit-flip and t-depolarizing noise channels, while for t-phase-flip and trit-phase-flip channels, such enhancement only occurs below certain noise thresholds. These findings provide theoretical insights for future studies in high-dimensional quantum communication and can serve as valuable guidance for improving the experimental implementation of CQT protocols.

Data availability statement

All data that support the findings of this study are included within the article (and any supplementary files).

Funding

This work is supported by the Kashi University Flexible Introduction Research Initiation Fund (No. 022024077), by the Kashi University School-level Research Project (Nos.(2023)1835, (2024)2923). Supported by the Natural Science Foundation of Xinjiang Uygur Autonomous Region (No. 2024D01A10). Supported by the Scientific Research Project of the Fundamental Research Funds for Higher Education Institutions in Xinjiang Uygur Autonomous Region (No. XJEDU2025P076). Supported by the Special project of Yili Normal University to improve comprehensive strength of disciplines (No. 22XKZZ18), Supported by the Yili Normal University scientific research innovation team plan project (No. CXZK2021015), and Supported by the Yili Science and Technology Planning Project (No. YZ2022B036).

Author contributions

In fact, all authors have made significant contributions to this paper. All authors have read and agreed to the published version of the manuscript.

Conflicts of interest

No potential conflict of interest was reported by the authors. All authors of this manuscript have read and approved the final version submitted and contents of this manuscript have not been copyrighted or published previously and is not under consideration for publication elsewhere.

References

[1] Nielsen M A and Chuang I L 2010 *Quantum Computation and Quantum Information* (Cambridge University Press) (https://doi.org/10.1007/s10773-023-05522-6)
[2] Furusawa A 2010 Quantum teleportation and quantum information processing *Laser Science to Photonic Applications* (IEEE) pp 1–2
[3] Barenco A and Ekert A K 1995 Dense coding based on quantum entanglement *J. Mod. Opt.* **42** 1253–9
[4] Bennett C H and Brassard G 2014 Quantum cryptography: Public key distribution and coin tossing *Theor. Comput. Sci.* **560** 7–11
[5] Ekert A K 1991 Quantum cryptography based on Bell's theorem *Phys. Rev. Lett.* **67** 661
[6] Peng J-Y and He Y 2019 Annular controlled teleportation *Int. J. Theor. Phys.* **58** 3271–81
[7] Bacon D, Kempe J, Lidar D A and Whaley K B 2000 universal fault-tolerant quantum computation on decoherence-free subspaces *Phys. Rev. Lett.* **85** 1758
[8] Aspect A, Grangier P and Roger G 1982 Experimental realization of Einstein-Podolsky-Rosen-Bohm Gedanken experiment: a new violation of Bell's inequalities *Phys. Rev. Lett.* **49** 91
[9] Bennett C H, Brassard G, Crépeau C, Jozsa R, Peres A and Wootters W K 1993 Teleporting an unknown quantum state via dual classical and Einstein-Podolsky-Rosen channels *Phys. Rev. Lett.* **70** 1895
[10] Bouwmesster D, Pan J W, Eibl M, Weinfurter H, Zeilinger A and Mattle K 1997 Experimental quantum teleportation *Nature* **390** 575–9
[11] Ren J-G *et al* 2017 Ground-to-satellite quantum teleportation *Nature* **549** 70–73
[12] Joo J, Park Y-J, Oh S and Kim J 2003 Quantum teleportation via a W state *New J. Phys.* **5** 136
[13] Yang K, Huang L, Yang W and Song F 2009 Quantum teleportation via GHZ-like state *Int. J. Theor. Phys.* **48** 516–21
[14] Nie S S *et al* 2008 Controlled teleportation using four-particle cluster state *Commun. Theor. Phys.* **50** 633–6
[15] Zha X-W *et al* 2013 Bidirectional quantum controlled teleportation via five-qubit cluster state *Int. J. Theor. Phys.* **52** 1740–4
[16] Aliloute S, Allati A E and Aouadi I E 2021 Bidirectional teleportation using coherent states *Quantum Inf. Process.* **20** 29
[17] Chen J *et al* 2020 Bidirectional quantum teleportation by using a four-qubit GHZ state and two Bell states *IEEE Access* **8** 1–1
[18] Hassanpour S and Houshmand M 2016 Bidirectional teleportation of a pure EPR state by using GHZ states *Quantum Inf. Process.* **15** 905–12
[19] Peng J-Y, Bai M and Mo Z-W 2016 Bidirectional quantum states sharing *Int. J. Theor. Phys.* **55** 2481–9
[20] Chen Y 2014 Bidirectional controlled quantum teleportation by using five-qubit entangled state *Int. J. Theor. Phys.* **53** 1454–8
[21] Peng J, Liu M, Tang J, Yang Z and Zhang Z 2024 Controlled cyclic quantum teleportation of unknown single-qutrit states *Int. J. Quantum Inf.* **22** 2350045
[22] Wu F, Bai M-Q, Zhang Y-C, Liu R-J and Mo Z-W 2020 Cyclic quantum teleportation of an unknown multi-particle high-dimension state *Mod. Phys. Lett. B* **34** 2050073
[23] Sun S and Zhang H 2020 Deterministic quantum cyclic controlled teleportation of arbitrary multi-qubit states using multi-qubit partially entangled channel *Mod. Phys. Lett. A* **35** 2050204
[24] Huang D Y, Zhou R G and Xu R Q 2023 Symmetric cyclic controlled quantum teleportation of three-qubit state by a nineteen-qubit entangled state *Int. J. Theor. Phys.* **63** 1
[25] Luo Y-H *et al* 2019 Quantum teleportation in high dimensions *Phys. Rev. Lett.* **123** 070505
[26] Horoshko D B, Patera G and Kolobov M I 2019 Quantum teleportation of qudits by means of generalized quasi-Bell states of light *Opt. Commun.* **447** 67
[27] Ma P-C, Chen G-B, Li X-W and Zhan Y-B 2018 Bidirectional Controlled Quantum Teleportation in the Three-dimension System *Int. J. Theor. Phys.* **57** 2233
[28] Hu X M *et al* 2020 Experimental high-dimensional quantum teleportation *Phys. Rev. Lett.* **125** 230501
[29] Zhou L *et al* 2024 Experimental realization of a three-photon asymmetric maximally entangled state and its application to quantum state transfer *Sci. Adv.* **10** 7
[30] Sephton B *et al* 2023 Quantum transport of high-dimensional spatial information with a nonlinear detector *Nat. Commun.* **14** 8243
[31] Bianchi L, Marconi C, Guarda G and Bacco D 2025 Nonlinear protocol for high-dimensional quantum teleportation *Phys. Rev. A* **112** 012615
[32] Brub D and Macchiavello C 2002 Optimal eavesdropping in cryptography with three-dimensional quantum states *Phys. Rev. Lett.* **88** 127901–127901
[33] Klimov A B, Guzmán R, Retamal J C and Saavedra C 2003 Qutrit quantum computer with trapped ions *Phys. Rev. A* **67** 062313

[34] Jiang S, Zhao B and Liang X 2021 Controlled quantum teleportation of an unknown single-qutrit state in noisy channels with memory *Chin. Phys. B* **30** 060303
[35] Oh S, Lee S and Lee H-W 2002 Fidelity of quantum teleportation through noisy channels *Phys. Rev. A* **66** 22316
[36] Peng J-Y and Xiang Y 2021 Bidirectional remote state preparation in noisy environment assisted by weak measurement *Opt. Commun.* **499** 127285
[37] Hou K, Bao D-Q, Zhu C-J and Yang Y-P 2019 Controlled teleportation of an arbitrary two-qubit entanglement in noises environment *Quantum Inf. Process.* **18** 104
[38] He L-M, Wang N and Zhou P 2020 Effect of quantum noise on teleportation of an arbitrary single-qubit state via a triparticle W state *Int. J. Theor. Phys.* **59** 1081–98
[39] Singh U, Mishra U and Dhar H S 2014 Enhancing robustness of multiparty quantum correlations using weak measurement *Ann. Phys., NY* **350** 50–68
[40] Peng J-Y and Xiang Y 2021 Multiparty quantum rotation operation sharing *Int. J. Theor. Phys.* **60** 3771–82
[41] Pan J-W *et al* 2001 Entanglement purification for quantum communication *Nature* **410** 1067–70
[42] Ren B-C, Du F-F and Deng F-G 2014 Two-step hyperentanglement purification with the quantum-state-joining method *Phys. Rev. A* **90** 052309
[43] Fonseca A 2019 High-dimensional quantum teleportation under noisy environments *Phys. Rev. A* **100** 062311
[44] Xiao X , Lu T-X , Li Y-L 2025 Enhanced high-dimensional teleportation in correlated amplitude damping noise by weak measurement and environment-assisted measurement *Quantum Inf. Process.* **24** 16
[45] Dakir Y, Slaoui A, Mohamed A-B A, Laamara R A and Eleuch H 2023 Quantum teleportation and dynamics of quantum coherence and metrological non-classical correlations for open two-qubit systems *Sci. Rep.* **13** 20526
[46] Kim H E and Jeong K 2024 Port-based entanglement teleportation via noisy resource states *Phys. Scr.* **99** 14
[47] Macchiavello C and Palma G M 2001 Entanglement enhanced information transmission over a quantum channel with correlated noise *Phys. Rev. A* **65** 882–6
[48] D'Arrigo A, Benenti G, Falci G and Macchiavello C 2015 Information transmission over an amplitude damping channel with an arbitrary degree of memory *Phys. Rev. A* **92** 062342
[49] Guo Y-N, Tian Q-L, Zeng K and Chen P-X 2020 Fidelity of quantum teleportation in correlated quantum channels *Quantum Inf. Process.* **19** 1–12
[50] Li Y-L, Zu C-J, Wei D-M and Wang C-M 2019 Correlated effects in Pauli channels for quantum teleportation *Int. J. Theor. Phys.* **58** 1350
[51] Zhang Z H and Sun M 2020 Enhanced deterministic joint remote state preparation under Pauli channels with memory *Phys. Scr.* **95** 055107
[52] Xu R, Zhou R-G, Li Y, Jiang S and Ian H 2022 Enhancing robustness of noisy qutrit teleportation with Markovian memory *EPJ Quantum Technol.* **9** 1–17
[53] Chen S and Gong W 2025 Efficient Pauli channel estimation with logarithmic quantum memory *PRX Quantum* **6** 020323
[54] Zhou H 2024 Asymmetric cyclic controlled quantum teleportation via multiple-qubit entangled state in a noisy environment *Entropy* **26** 1108
[55] Liu X S, Long G L, Tong D M and Li F 2002 General scheme for superdense coding between multiparties *Phys. Rev. A* **65** 022304
[56] Karimipour V, Bahraminasab A and Bagherinezhad S 2002 Entanglement swapping of generalized cat states and secret sharing *Phys. Rev. A* **65** 042320
[57] Karimipour V, Bagherinezhad S and Bahraminasab A 2001 Quantum key distribution for d-level systems with generalized Bell states *Phys. Rev. A* **65** 066302
[58] Zyczkowski K and Sommers H-J 2001 Induced measures in the space of mixed quantum states *J. Phys. A: Math. Gen.* **34** 7111